J|A|C|S ARTICLES

Published on Web 12/19/2008

Multiphoton Infrared Initiated Thermal Reactions of Esters: Pseudopericyclic Eight-Centered *cis*-Elimination

Hua Ji, Li Li,[†] Xiaolian Xu,[‡] Sihyun Ham,[§] Loubna A. Hammad,[¶] and David M. Birney*

Department of Chemistry and Biochemistry, Texas Tech University, Lubbock, Texas 79409-1061

Received June 24, 2008; E-mail: david.birney@ttu.edu

Abstract: Multiphoton infrared absorption from a focused, pulsed CO_2 laser was used to initiate gas-phase thermal reactions of *cis*- and *trans*-3-penten-2-yl acetate. By varying the helium buffer gas pressure, it was possible to deduce the product distribution from the initial unimolecular reactions, separate from secondary reactions in a thermal cascade. Thus, *trans*-3-penten-2-yl acetate gives 54 ± 5% of β-elimination to give *trans*-1,3-pentadiene, 40 ± 3% of [3,3]-sigmatropic rearrangement to give *cis*-3-penten-2-yl acetate and 6 ± 4% of *cis*-1,3-pentadiene. Similar irradiation of *cis*-3-penten-2-yl acetate gives 45 ± 1% of β-elimination to give *cis*-1,3-pentadiene, 32 ± 2% of [3,3]-sigmatropic rearrangement to give *trans*-3-penten-2-yl acetate and 23 ± 2% of *trans*-1,3-pentadiene. The latter process is an eight-centered δ-elimination, which is argued to be a pseudopericyclic reaction. Although β-eliminations have been suggested to be pericyclic, B3LYP/6−31G(d,p), MP2 and MP4 calculations suggest that both β- and δ-eliminations, as well as [3,3]-sigmatropic rearrangements of esters are primarily pseudopericyclic in character, as judged by both geometrical, energetic and transition state aromaticity (NICS) criteria. Small distortions from the ideal pseudopericyclic geometries are argued to reflect small pericyclic contributions. It is further argued that when both pericyclic and pseudopericyclic orbital topologies are allowed and geometrically feasible, the calculated transition state may be the result of proportional mixing of the two states; this offers an explanation of the range of pseudopericyclic and pericyclic characters found in related reactions.

Introduction

A pseudopericyclic reaction is a concerted reaction in which bond changes occur around a ring, but which lacks the cyclic orbital overlap that is characteristic of a pericyclic reaction.[1,2] "A pseudopericyclic reaction may be orbital symmetry allowed... regardless of the number of electrons involved."[1a] In support of this bold statement, we have reported ab initio[1d] and density functional theory (DFT) calculations[1e] which indicate that [1,3], [3,3], and [3,5] sigmatropic rearrangements of esters are all pseudopericyclic and allowed. These are consistent with the observed competition between [3,3] and [3,5] rearrangements of **1** that favors the [3,5] product **2** (eq 1).[1e] We now report that the same is true of ester eliminations, namely that eight-

[†] Present address: Department of Chemistry, Purdue University, 560 Oval Drive, West Lafayette, IN 47907-2084.

[‡] Present address: Lexicon Pharmaceuticals, 350 Carter Road, Princeton, New Jersey 08540.

[§] Present address: Department of Chemistry, Sookmyung Women's University, Seoul 140-742, Republic of Korea.

[¶] Present address: Department of Chemistry, Indiana University, 800 E. Kirkwood Ave., Bloomington, IN 47405-7102.

(1) (a) Ross, J. A.; Seiders, R. P.; Lemal, D. M. *J. Am. Chem. Soc.* **1976**, *98*, 4325–4327. (b) Birney, D. M.; Wagenseller, P. E. *J. Am. Chem. Soc.* **1994**, *116*, 6262–6270. (c) Birney, D. M.; Ham, S.; Unruh, G. R. *J. Am. Chem. Soc.* **1997**, *119*, 4509–4517. (d) Birney, D. M.; Xu, X.; Ham, S. *Angew. Chem., Int. Ed.* **1999**, *38*, 189–193. (e) Quideau, S.; Looney, M. A.; Pouységu, L.; Ham, S.; Birney, D. *Tetrahedron Lett.* **1999**, *40*, 615–618. (f) Shumway, W. W.; Dalley, N. K.; Birney, D. M. *J. Org. Chem.* **2001**, *66*, 5832–5839. (g) Wei, H.-X.; Zhou, C.; Ham, S.; White, J. M.; Birney, D. M. *Org. Lett.* **2004**, *6*, 4289–4292. (h) Gudipati, I. R.; Sadasivam, D. V.; Birney, D. M. *Green Chem.* **2008**, *10*, 283–285. (i) Sadasivam, D. V.; Birney, D. M. *Org. Lett.* **2008**, *10*, 245–248.

(2) (a) Huisgen, R. *Angew. Chem., Int. Ed. Engl.* **1980**, *19*, 947–973. (b) Fabian, W. M. F.; Kappe, C. O.; Bakulev, V. A. *J. Org. Chem.* **2000**, *65*, 47–53. (c) de Lera, A. R.; Alvarez, R.; Lecea, B.; Torrado, A.; Cossío, F. P. *Angew. Chem., Int. Ed. Engl.* **2001**, *40*, 557–561. (d) Rodríguez-Otero, J.; Cabaleiro-Lago, E. M. *Angew. Chem., Int. Ed.* **2002**, *41*, 1147–1150. (e) de Lera, A. R.; Cossío, F. P. *Angew. Chem., Int. Ed.* **2002**, *41*, 1150–1152. (f) Rodríguez-Otero, J.; Cabaleiro-Lago, E. M.; Hermida-Ramón, J. M.; Peña-Gallego, A. *J. Org. Chem.* **2003**, *68*, 8823–8830. (g) Cabaleiro-Lago, E. M.; Rodríguez-Otero, J.; González-López, I.; Peña-Gallego, A.; Hermida-Ramón, J. M. *J. Phys. Chem. A* **2005**, *109*, 5636–5644. (h) Zora, M. *J. Org. Chem.* **2004**, *69*, 1940–1947. (i) Cabaleiro-Lago, E. M.; Rodríguez-Otero, J.; Varela-Valera, S. M.; Peña-Gallego, A.; Hermida-Ramón, J. M. *J. Org. Chem.* **2005**, *70*, 3921–3928. (j) Cabaleiro-Lago, E. M.; Rodríguez-Otero, J.; Garcia-López, R. M.; Peña-Gallego, A.; Hermida-Ramón, J. M. *Chem.−Eur. J.* **2005**, *11* (20), 5966–5974. (k) Fukushima, K.; Iwahashi, H. *Heterocycles* **2005**, *65*, 2605–2618. (l) López, C. S.; Faza, O. N.; Cossío, F. P.; York, D. M.; de Lera, A. R. *Chem.−Eur. J.* **2005**, *11*, 1734–1738. (m) Alajarin, M.; Ortin, M.-M.; Sanchez-Andrada, P.; Vidal, A. *J. Org. Chem.* **2006**, *71*, 8126–8139. (n) Sheikhshoaie, I.; Belaj, F.; Fabian, W. M. F. *J. Mol. Struct.* **2006**, *794*, 244–250. (o) Fukushima, K.; Iwahashi, H. *Chem. Lett.* **2006**, *35*, 1242–1243. (ii) Kruger, H. G.; Mdluli, P.; Power, T. D.; Raasch, T.; Singh, A. *J. Mol. Struct. THEOCHEM* **2006**, *771*, 165–170. (p) Rode, J. E.; Dobrowoski, J. C. *J. Phys. Chem. A* **2006**, *110*, 3723–3737. (q) George, L.; Netsch, K. P.; Penn, G.; Kollenz, G.; Wentrup, C. *Org. Biomol. Chem.* **2006**, *4*, 558–564. (r) Peña-Gallego, A.; Rodríguez-Otero, J.; Cabaleiro-Lago, E. M. *Tetrahedron* **2007**, *63*, 4937–4943. (s) Chamorro, E.; Notario, R.; Santos, J. C.; Perez, P. *Chem. Phys. Lett.* **2007**, *443*, 136–140. (t) Peña-Gallego, A.; Rodríguez-Otero, J.; Cabaleiro-Lago, E. M. *J. Phys. Chem. A* **2007**, *111*, 2935–2940. (u) Rode, J. E.; Dobrowolski, J. C. *Chem. Phys. Lett.* **2007**, *449*, 240–245. (v) Calvo-Losada, S.; Sanchez, J. J. Q. *J. Phys. Chem. A* **2008**, *112*, 8164–8178.

10.1021/ja804812c CCC: $40.75

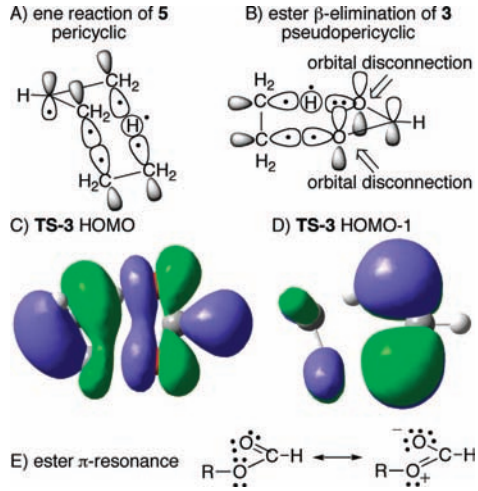

Figure 1. (A) Qualitative transition state orbital overlap in the pericyclic hydrocarbon retro-ene reaction of 1-pentene (**5**) and (B) in the planar, pseudopericyclic β-elimination of ethyl formate (**3**). (C, D) HOMO (in-plane) and HOMO-1 (out-of-plane) of the B3LYP/6−31G(d,p) transition state for β-elimination of **3**, (**TS-3**, after reference.[7b] (E) Ester resonance.[9] Note that the ester β-elimination could alternatively involve orbital overlap with the ester π-system as in Figure 1A; this would disrupt the ester π-resonance that is preserved in the pseudopericyclic orbital topology in 1B.

centered δ-eliminations (e.g., of **4**, eq 2b) are competitive with the more familiar β-eliminations (e.g., of **3**, eq 2a).[3]

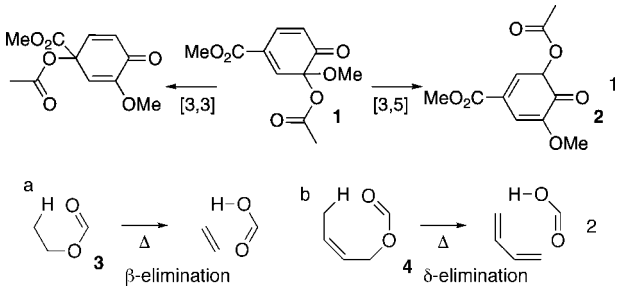

It is well-known that pyrolysis of esters with a β-hydrogen (e.g., ethyl formate, **3**) leads to stereospecific *cis*-elimination via a six-centered transition state (β-elimination, eq 2a).[4] This synthetically useful, textbook reaction has often been described as a six-electron concerted process that is fundamentally the same as a retro-ene reaction.[5] Shortly after the publication of the Woodward−Hoffmann rules it was explicitly described as an allowed σ^2CH + π^2CO + σ^2CO reaction.[5a] In light of the synthetic and theoretical importance of this reaction, it is not surprising there have been both semiempirical[6] and quantum chemical[7] calculations of β-elimination from ethyl formate (**3**) and of more complex esters. The calculated transition state has been described as "'aromatic' in that it involves six electrons in a six-membered cyclic structure."[6a] Although this mechanistic description is familiar and seems reasonable, it is not consistent with the fact that at all levels of theory, the transition state is planar, or close to planar.[6,7] This geometry is in qualitative contrast to the calculated transition state for the hydrocarbon retro-ene reaction of 1-pentene (**5**, eq 3), which has a nonplanar transition state to allow for π-orbital overlap in a pericyclic transition state, as illustrated in Figure 1A.[8]

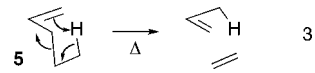

The details of possible transition states will be discussed in more detail below in the context of new computational results. Briefly, a planar transition state geometry for an ester β-elimination is possible because the ester π-system is disconnected from the in-plane σ-system as shown in Figure 1B. This planar transition state transfers a proton to an ester carbonyl lone pair and the breaking bond becomes a lone pair on the acid. The HOMO and HOMO-1 for the planar transition state for β-elimination from **3** (**TS-3**, B3LYP/6−31G(d,p)[7b]) are shown in Figure 1C and D. The in-plane and out-of plane systems remain orthogonal and therefore cannot have cyclic orbital overlap involving the π-system;[10] thus, the transition state can neither be aromatic nor antiaromatic.[11] Nor can it be discussed in terms of the Woodward−Hoffmann rules[12] because it has neither suprafacial nor antarafacial orbital overlap. Rather, this orbital topology corresponds to a pseudopericyclic transition state, as first described by Lemal[1a] and as subsequently discussed by us[1b−i] and others.[2] The lack of cyclic orbital overlap in pseudopericyclic reactions may have three experimental consequences: (1) such reactions are allowed regardless of the

(3) A preliminary communication of computational results on model systems has been presented: Birney, D. M.; Xu, X.; Ham, S. *Pseudopericyclic Reactions of Esters: Eight-Centered Cis Elimination is Allowed*; Abstracts of National Meeting of The American Chemical Society, Boston, MA, 1998.

(4) (a) DePuy, C. H.; King, R. W. *Chem. Rev.* **1960**, *60*, 431–457. (b) Benson, R. E.; McKusick, B. C.; Grummitt, O.; Budewitz, E. P.; Chudd, C. C. *Org. Synth. Coll.* **1963**, *4*, 746. (c) Smith, G. G.; Kelly, F. W. *Prog. Phys. Org. Chem.* **1971**, *8*, 75–234.

(5) (a) Caserio, M. C. *J. Chem. Educ.* **1971**, *48*, 782–790. (b) Alder, R. W.; Baker, R.; Brown, J. M. Stabilized cyclically conjugated transition states. *Mechanism in Organic Chemistry*, 1st ed.; John Wiley & Sons: London, 1971; p 239, "stabilized cyclically conjugated transition-states". (c) Pearson, R. G., A six-electron TS. *Symmetry Rules for Chemical Reactions*, 1st ed.; John Wiley and Sons: New York, 1976; p 368, "a six-electron TS". (d) Gilchrist, T. L.; Storr, R. C. *Organic reactions and orbital symmetry*, 1st ed.; Cambridge University Press: Cambridge, 1979; Section 7.8, p 292, "other six-electron pericyclic processes". (e) Fleming, I. It must be all-suprafacial and it is therefore fundamentally a retro-ene reaction. *Pericyclic Reactions*, 1st ed.; Oxford University Press: Oxford, 1999; p 87, "it must be all-suprafacial and it is therefore fundamentally a retro-ene reaction".

(6) (a) Lee, I.; Cha, O. J.; Lee, B.-S. *J. Phys. Chem.* **1990**, *94*, 3926–3930. (b) Hamon, L.; Levisalles, J.; Pascal, Y.-L. *Tetrahedron* **1994**, *50*, 161–170.

(7) (a) Bohm, S.; Skancke, P. N. *Int. J. Quantum Chem.* **1991**, *40*, 491–500. (b) Erickson, J. A.; Kahn, S. D. *J. Am. Chem. Soc.* **1994**, *116*, 6271–6276. (c) Speybroeck, V. V.; Martele, Y.; Schacht, E.; Waroquier, M. *J. Phys. Chem. A* **2002**, *106*, 12370–12375. (d) Notario, R.; Quijano, J.; Quijano, J. C.; Gutiérrez, L. P.; Suárez, W. A.; Sánchez, C.; León, L. A.; Chamorro, E. *J. Phys. Chem. A* **2002**, *106*, 4377–4383. (e) Hermida-Ramón, J. M.; Rodríguez-Otero, J.; Cabaleiro-Lago, E. M. *J. Phys. Chem. A* **2003**, *107*, 1651–1654. (f) Silva, A. M. *Chem. Phys. Lett.* **2007**, *439*, 8–13.

(8) (a) Loncharich, R. J.; Houk, K. N. *J. Am. Chem. Soc.* **1987**, *109*, 6947–6952. (b) Deng, Q.; Thomas, B. E. IV.; Houk, K. N.; Dowd, P. *J. Am. Chem. Soc.* **1997**, *119*, 6902–6908. (c) Sakai, S. *J. Phys. Chem. A* **2006**, *110*, 12891–12899.

(9) Wiberg has advanced an alternative explanation for the planarity of esters; see: Wiberg, K. B.; Laidig, K. E. *J. Am. Chem. Soc.* **1987**, *109*, 5935–5943, and references therein.

(10) Note that there is some cyclic overlap between non-adjacent atoms in the in-plane system (Figure 1C).

(11) (a) Dewar, M. J. S. *Angew. Chem. Int., Ed. Engl.* **1971**, *10*, 761. (b) Zimmerman, H. E. *Acc. Chem. Res.* **1971**, *4*, 272. (c) Schleyer, P. v. R.; Maerker, C.; Dransfeld, A.; Jiao, H.; Hommes, N. J. R. v. E. *J. Am. Chem. Soc.* **1995**, *118*, 6317–6318. (d) Morao, I.; Lecea, B.; Cossio, F. P. *J. Org. Chem.* **1997**, *62*, 7033–7036. (e) Herges, R.; Geuenich, D. *J. Chem. Phys. A* **2001**, *105*, 3214–3220.

(12) Woodward, R. B.; Hoffmann, R., *The Conservation of Orbital Symmetry.* ed.; Verlag Chemie, GmbH: Weinheim, 1970.

Scheme 1

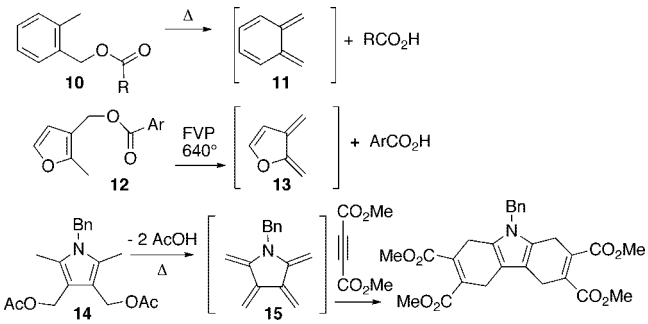

number of atoms involved,[1e,f,i] (2) the transition states can be planar, in contrast to the nonplanar ones for pericyclic reactions,[1f,g] (3) the barrier heights can be lower than a competing pericyclic alternative.[1b,c] Pseudopericyclic reactions are expected not to show the calculated transition state aromaticity associated with pericyclic reactions.[2d,m,11c−e]

If the 6-centered transition state for β-elimination is pseudopericyclic, then our qualitative prediction is that the vinylogous δ-elimination is also allowed via an 8-centered transition state. Prior to the Woodward/Hoffmann rules, there were a number of experimental studies that gave serious consideration to the possibility of δ-eliminations of esters, including some of the earliest experimental studies of ester pyrolyses. In 1956, Bailey et al. studied the products obtained by flash vacuum pyrolysis of *cis*-2-buten-1,4-diol acetate (**6**, eq 4).[13] They obtained a 26% yield of the formal δ-elimination product (**7**) and a 20% yield of rearranged diacetate (**8**), along with 24% of recovered **6**. They commented that **7** could be formed by rearrangement to **8**, followed by 6-centered elimination but that their results could not rule out a small amount of a direct eight-centered elimination. Interestingly, there was none of the isomeric diene **9** that could, in principle also be formed by elimination from **8**.

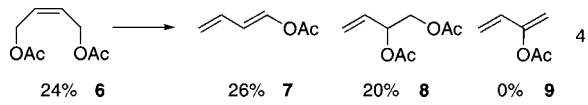

A number of ester eliminations that lead to ortho-xylylene and related species have also been studied, as shown in Scheme 1. These include eliminations to form *ortho*-xylylene (**11**),[14] as well as heteroaromatic analogs[15] including the furyl derivative **13**.[14] The intermediates were not isolated, but were trapped with a variety of dienophiles. The pyrrole derivative **14** also gave trapping products that would be consistent with the radiallene derivative **15** as an intermediate, although stepwise elimination, trapping, elimination and trapping is also possible.[15c] Tranhanovsky et al.[14] recognized that there were two possible mechanisms for such a reaction, (1) direct δ-elimination via an eight-centered transition state, or (2) a two-step process, consisting of a [3,3] rearrangement followed by a more conventional β-elimination. The rearrangement in the two-step process disrupts the aromatic or heteroaromatic ring, favoring, but not requiring the direct δ-elimination.

(13) Bailey, W. J.; Barclay, R., Jr. *J. Org. Chem.* **1956**, *21*, 328–331.
(14) Trahanovsky, W. S.; Cassady, T. J.; Woods, T. L. *J. Am. Chem. Soc.* **1981**, *103*, 6691–6695.
(15) (a) Potter, A. J.; Storr, R. C. *Tetrahedron Lett.* **1994**, *35*, 5293–5296. (b) Chauhan, P. M. S.; Crew, A. P. A.; Jenkins, G.; Storr, R. C.; Walker, S. M.; Yelland, Y. *Tetrahedron Lett.* **1990**, *31*, 1487–1490. (c) Vessels, J. T.; Janicki, S. Z.; Petillo, P. A. *Org. Lett.* **2000**, *2*, 73–76.

Scheme 2

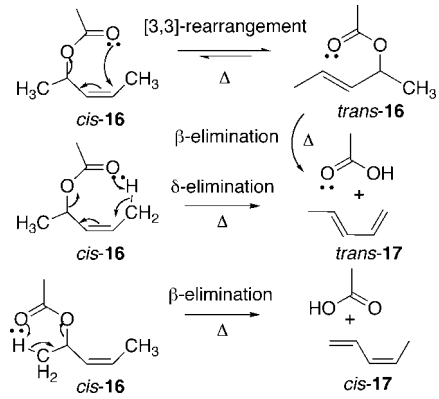

The pyrolyses of several allylic acetates have been studied by Lewis et al. and the kinetics for racemization have been measured.[16] Of particular relevance to this work is the rearrangement of optically active *trans*-**16** shown in equation 5. Rearrangement leads to racemization with an $E_a = 38.8 \pm 0.5$ kcal/mol. This is faster than, but competitive with elimination to form *trans*-**17**. Because of the double bond geometry in *trans*-**16**, an eight-centered elimination is geometrically disfavored and the formation of *trans*-**17** can be assumed to involve only β-elimination. Isomerization to *cis*-**16** is also observed, but is a minor pathway.

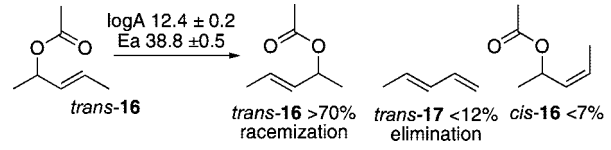

Results and Discussion

The pyrolysis of *cis*-3-penten-2-yl acetate (*cis*-**16**) was studied in this work because it provides a stringent test of the qualitative prediction that δ-elimination via an eight-centered transition state is allowed. This substrate (*cis*-**16**) has the potential to undergo three reactions, both β- and δ-eliminations as well as a [3,3]-sigmatropic rearrangement, with little or no steric or energetic bias toward any one pathway (Scheme 2).[17] A [3,3]-sigmatropic rearrangement would be expected to give the more stable *trans*-3-penten-2-yl acetate (*trans*-**16**) in preference to the degenerate rearrangement to give *cis*-**16**; this expectation is confirmed by the computational studies described below. β-Elimination of acetate from *cis*-**16** could only give *cis*-1,3-pentadiene (*cis*-**17**). If the δ-elimination is allowed and competitive, the geometry of *cis*-**16** would permit it; thermodynamic control would also be expected to give the more stable *trans*-1,3-pentadiene (*trans*-**17**) in preference to *cis*-**17**; this is similarly in accord with computations, below. However, observation of *trans*-**17** from a conventional pyrolysis does not require the concerted δ-elimination; *trans*-**17** can be formed via sequential rearrangement to *trans*-**16** followed by β-elimination. Nevertheless, we anticipated that we could distinguish these two pathways for formation

(16) Lewis, E. S.; Hill, J. T.; Newman, E. R. *J. Am. Chem. Soc.* **1968**, *90*, 662–668.
(17) Additional transition states were considered in the computational studies described below and in the Supporting Information. Their energies are sufficiently high that these processes do not need to be considered in this context.

Scheme 3. MP-IR Initiated Reaction of *cis*-**16**[a]

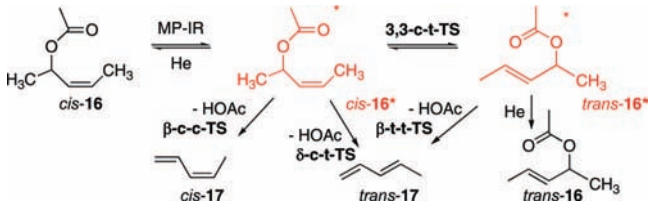

[a] Vibrationally excited molecules are shown in red and designated by an asterisk.

of *trans*-**17** by multiphoton infrared (MP-IR) photolysis/thermolysis, as described below.

Multiphoton Infrared Photolysis/Thermolysis (MP-IR). We[18] and others[19] have previously used multiphoton infrared photolysis/thermolysis to identify first-formed intermediates in other thermal reaction cascades and it appeared to be a promising technique to answer this question as well.[18b] This technique has been described in detail elsewhere;[20] briefly, a pulsed infrared laser is tuned to a frequency where a compound of interest has an IR absorption. In the gas phase, absorption of one IR photon is followed by intramolecular vibrational relaxation (IVR); this process is generally enhanced by molecular collisions. This allows for the absorption of another photon; within a typical laser pulse of approximately 100 ns, a molecule can thus absorb multiple photons and be heated sufficiently to undergo relatively high barrier reactions. This heating is generally assumed to give a molecule with a random (Boltzmann) energy distribution. However, any molecule that does not absorb the IR photons cannot be heated. Thus a nonabsorbing buffer gas can rapidly cool initial products in competition with a secondary thermal reaction. MP-IR reactions can be carried out at pressures up to approximately 100 torr, which balances the increased IR absorbance due to collision-induced IVR with the increased cooling at higher pressures.

Yuan T. Lee has used MP-IR to initiate the decomposition of ethyl acetate in a molecular beam/TOF mass spectrometer experiment.[19c] The major reaction channel is the β-elimination to give ethene and acetic acid. Under the low-pressure conditions of this experiment, the acetic acid undergoes some secondary thermolysis to give ketene and water. A minor pathway is homolytic fragmentation to give ethyl radical, methyl radical, and CO_2.

Applying the MP-IR technique to the thermal reactions of *cis*-**16** suggests a reaction scheme as shown in Scheme 3. MP-IR heating of *cis*-**16** leads to a molecule with sufficient internal energy (designated by *, *cis*-**16***) to react via the transition states,[21] **3,3-c-t-TS**, ***β*-c-c-TS** or possibly ***δ*-c-t-TS**, in competition with collisional cooling from the helium buffer gas. Conservation of energy dictates that rearrangement of *cis*-**16*** produces *trans*-**16***, also with sufficient internal energy to likely undergo β-elimination via ***β*-t-t-TS**. However, collisional cooling of *trans*-**16*** will occur in competition with the elimination. Since the collisional cooling of *trans*-**16*** is a bimolecular process and the β-elimination to form *trans*-**17** is unimolecular, these two processes can be distinguished. In the simplest analysis, if *trans*-**16** does not absorb at the wavelength of the IR photons, then it remains cool and unreactive. As will be shown below, *trans*-**16** does absorb at the IR wavelength and does react, but extrapolation to the initial reaction of *cis*-**16** removes this complication.

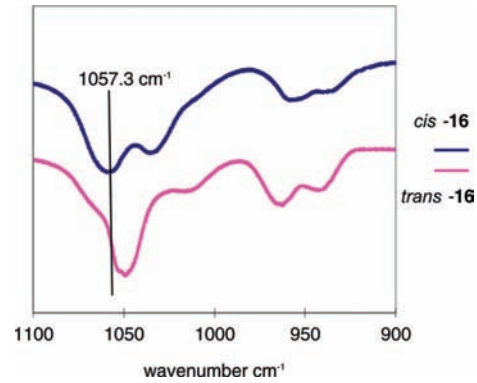

Figure 2. Gas phase (3 torr) IR spectra of *cis*-**16** and *trans*-**16** in the region of 1100 to 900 cm^{-1} (2 cm^{-1} resolution) and the laser line at 1057.3 cm^{-1} used for the MP-IR irradiation. The baselines are offset to show the spectra more clearly.

Experimental Methods

cis-3-Penten-2-yl acetate (*cis*-**16**)[16] was synthesized as outlined in equation 6;[22] full experimental details and spectroscopic characterization are provided in the Supporting Information. Following Henry,[22a] propynylmagnesium bromide was added to acetaldehyde to give the propargyl alcohol **18**[22a] and subsequent reduction with Lindlar's catalyst gave *cis*-3-penten-2-ol (**19**).[22a] Esterification[22b] with acetyl chloride gave *cis*-**16**.[22c] *trans*-3-Penten-2-yl acetate[22b,c] (*trans*-**16**) was synthesized by acetylation of commercially available *trans*-3-penten-2-ol.

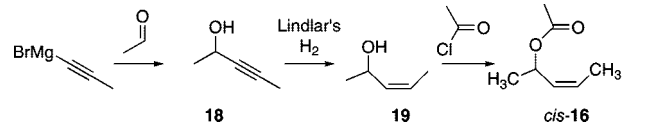

Our apparatus for MP-IR experiments has been previously described.[18] Briefly, a pulsed TEA CO_2 laser is focused by a ZnSe lens into a 10 cm gas cell fitted with NaCl windows and filled with 0.7 torr of *cis*-**16** and a known pressure of He buffer gas (0 to 20 torr). Comparison of the IR spectra of *cis*-**16** and *trans*-**16** with the emission lines available from the TEA CO_2 laser suggested that 1057.3 cm^{-1} would give stronger absorbance by *cis*-**16** relative to *trans*-**16** (Figure 2), so this wavelength was selected for this study. Based on B3LYP/6−31G(d,p) frequency calculations (vide infra), this corresponds to a C−O single bond stretch. This frequency is on the side of an absorption in *trans*-**16** that also is calculated to correspond to a C−O stretch. The laser frequency was measured using a CO_2 laser spectrum analyzer. The progress of the reaction was followed by IR spectroscopy. After 100 laser pulses, nitrogen was added to bring the cell to atmospheric pressure. The products

(18) (a) Unruh, G. R.; Birney, D. M. *J. Am. Chem. Soc.* **2003**, *125*, 8529–8533. (b) Li, L. *Elimination of cis-3-Penten-2-yl Acetate*. M.S. Thesis, Texas Tech University, Lubbock, TX, 2003.

(19) (a) Nguyen, H. H.; Danen, W. C. *J. Am. Chem. Soc.* **1981**, *103*, 6253–6255. (b) Danen, W. C.; Rio, V. C.; Setser, D. W. *J. Am. Chem. Soc.* **1982**, *104*, 5431–5440. (c) Hintsa, E. J.; Wodtke, A. M.; Lee, Y. T. *J. Phys. Chem.* **1988**, *92*, 5379–5387.

(20) (a) Bagratashvilli, V. N.; Letokhov, V. S.; Makarov, A. A.; Ryabov, E. A. *Laser Chem.* **1984**, *5*, 53–105. (b) Lupo, D. W.; Quack, M. *Chem. Rev.* **1987**, *87*, 181–216.

(21) Transition states related to **16** are designated as follows: first, the type of reaction is indicated, [3,3]-sigmatropic rearrangement, b-elimination or d-elimination, then *cis* or *trans* as related to the double bond geometries in reactants and products. For other transition states, the compound number of the starting material is also included.

(22) (a) Hamed, O.; Henry, P. M. *Organometallics* **1997**, *16*, 4903. (b) Bateson, J. H.; Quinn, A. M.; Smale, T. C.; Southgate, R. *J. Chem. Soc. Perkin Trans 1.* **1985**, 2219. (c) McKew, J. C.; Kurth, M. J. *J. Org. Chem.* **1993**, *58*, 4589–4595.

Scheme 4. MP-IR Initiated Reaction of *trans*-**16**

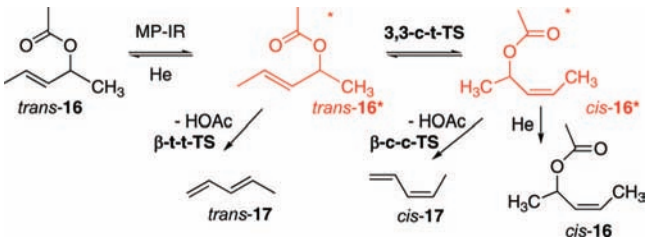

in the gas phase were directly injected into the GC and each experiment was analyzed in triplicate. The product ratios were corrected for FID response factors and are reported in the Supporting Information.

Experimental Results

The first experiment performed was a conventional flash vacuum pyrolysis of *cis*-**16** (containing 6% *trans*-**16**) at 400 °C. As expected, this gave a mixture of *trans*-**16** (19%) *cis*-**17** (13%) and *trans*-**17** (11%) along with unreacted *cis*-**16** (57%) This is consistent with Lewis' results,[16] in that all three products are formed. It does not address the question as to whether δ-elimination occurs via an eight-centered transition state; therefore the MP-IR experiments were undertaken. Significantly, *cis*-3-penten-2-ol (**19**) was recovered unchanged when it was submitted to the pyrolysis conditions, indicating that a 6-centered δ-elimination of water does not occur under these conditions.

The MP-IR induced reactions of both *cis*-**16** and *trans*-**16** were then studied. The results for *trans*-**16** are more straightforward and will be discussed first. The anticipated reactions are outlined in Scheme 4. The only mechanism for the formation of *cis*-**17** is the sequential process, rearrangement of *trans*-**16*** to *cis*-**16*** followed by β-elimination to give *cis*-**17**. In principle, it should be possible to completely quench the formation of *cis*-**17** at sufficiently high He pressures. In practice, increasing the He pressure also cools *trans*-**16*** and thus quenches all the reactions. Nevertheless, it is possible to extrapolate to infinite He pressure.

When *trans*-**16** (1.7 torr) was subjected to MP-IR irradiation at 1057.3 cm^{-1} at varying He pressures (0 to 20 torr) the anticipated products *trans*-**17**, *cis*-**17**, and *cis*-**16** were formed. In accord with Lee's MP-IR results on ethyl formate,[19c] ketene was also observed by in situ IR and by GC, however, because this was only a small quantity of a secondary product, it is not considered in the following discussion. The product distributions of *trans*-**17**, *cis*-**17**, and *cis*-**16** were analyzed as follows. The percent reaction was taken as the sum of the three products, divided by the sum of these products and unreacted *trans*-**16** (eq 7) Higher pressures of He as buffer gas led to lower overall percent reaction. The percent of each product was taken as the proportion of that product (*trans*-**17**, *cis*-**17**, or *cis*-**16**) divided by the sum of these three products (eq 8). The percent of each product as a function of percent reaction is shown in Figure 3.

$$\%\ \text{reaction} = \frac{\text{sum GC yields } \textit{cis}\text{-}\mathbf{16},\textit{cis}\text{-}\mathbf{17},\textit{trans}\text{-}\mathbf{17}}{\text{sum GC yields } \textit{trans}\text{-}\mathbf{16},\textit{cis}\text{-}\mathbf{16},\textit{cis}\text{-}\mathbf{17},\textit{trans}\text{-}\mathbf{17}} \quad (7)$$

$$\%\text{product} = \frac{\text{GC yield product}}{\text{sum GC yields } \textit{cis}\text{-}\mathbf{16},\textit{cis}\text{-}\mathbf{17},\textit{trans}\text{-}\mathbf{17}} \quad (8)$$

The results in Figure 3 are consistent with the qualitative reaction mechanism in Scheme 4. The proportion of *trans*-**17** as a percentage of products is relatively constant (extrapolating to 54 ± 5% of the initial reaction) as the He pressure is changed.

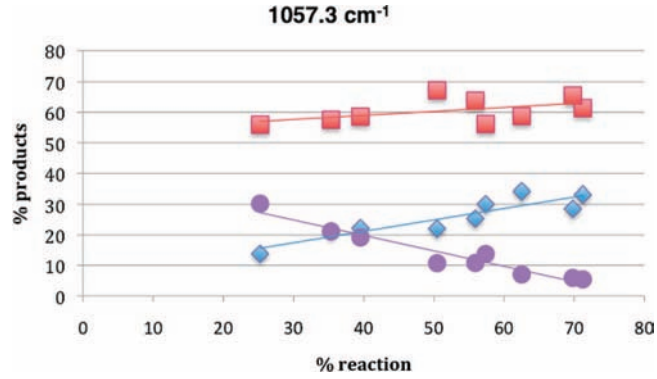

Figure 3. Product composition versus percent reaction of *trans*-**16** under MP-IR irradiation at 1057.3 cm^{-1}. Red squares are *trans*-**17**, blue diamonds are *cis*-**17** and purple circles are *cis*-**16**. The lines are a linear least-squares fit to the data; *trans*-**17**, $y = (0.13 \pm 0.09)x + (53.7 \pm 4.6)$; *cis*-**17**, $y = (0.37 \pm 0.07)x + (6.2 \pm 3.6)$; *cis*-**16**, $y = (-0.51 \pm 0.05)x + (40.1 \pm 2.8)$. See Scheme 4.

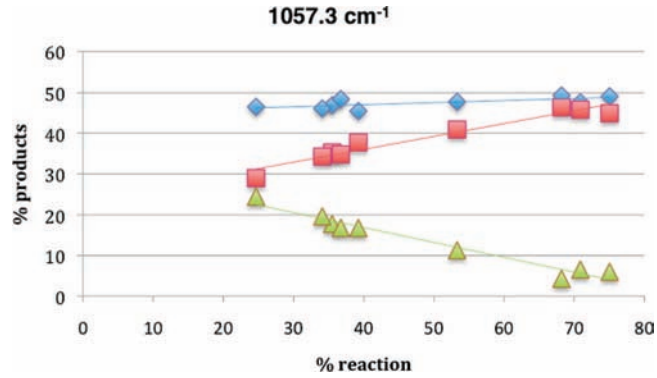

Figure 4. Product composition versus percent reaction of *cis*-**16** under MP-IR irradiation at 1057.3 cm^{-1}. Red squares are *trans*-**17**, blue diamonds are *cis*-**17** and green triangles are *trans*-**16**. The lines are a linear least-squares fit to the data; are *trans*-**17**, $y = (0.31 \pm 0.03)x + (23.4 \pm 1.5)$; *cis*-**17**, $y = (0.05 \pm 0.02)x + (45.0 \pm 1.0)$; *trans*-**16**, $y = -0.37 \pm 0.03)x + (31.6 \pm 1.5)$. See Scheme 3.

This is to be expected, as the only reaction that forms *trans*-**17** is one of the two reactions of *trans*-**16*** that lead directly to products, in a ratio determined by their respective unimolecular rate constants, and would be equally quenched by collisional cooling of *trans*-**16*** by He. In contrast, the percentage of the rearrangement product *cis*-**16** increases significantly; it extrapolates to 40 ± 3% with decreasing percent reaction (increasing He pressure). Concomitantly, the proportion of *cis*-**17** decreases; it extrapolates to close to zero (6 ± 4%) as the He pressure is increased. This is as expected if all of the *cis*-**17** is formed sequentially by rearrangement of *trans*-**16*** to *cis*-**16*** followed by β-elimination. This is significant because it demonstrates that the MP-IR technique, along with collisional cooling of hot intermediate species, is able to identify the contributions to the product ratio from the initial, unimolecular reactions, separate from a second, but likewise unimolecular step.

In light of this, a similar series of MP-IR experiments were performed on *cis*-**16**. The results were analyzed analogously to eq 7 and 8 for *trans*-**16** and are shown in Figure 4. The anticipated reaction mechanism is shown in Scheme 3. Briefly, we anticipate that some *trans*-**17** is formed in a stepwise process via *trans*-**16***; collisional cooling by added He buffer gas will increase the proportion of *trans*-**16** at the expense of *trans*-**17**. A Stern-Volmer plot of the *cis*-**16** reaction versus He pressure was linear, indicating that collisional cooling by He is occurring

Scheme 5. Transition States Calculated for Reactions of *cis*-**16** and *trans*-**16**[21a]

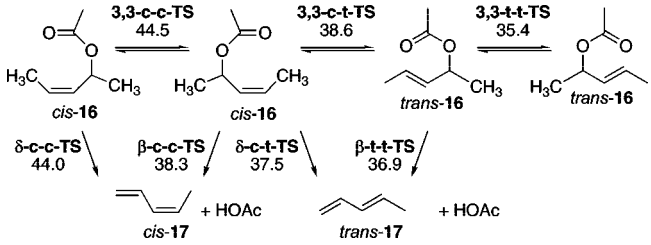

[a] Relative free energies (B3LYP/6-31G(d,p), 298.2 K) are in kcal/mol.

(Figure S8). However, any proportion of *trans*-**17** that may be formed directly from *cis*-**16*** via a δ-elimination cannot be affected by added He buffer gas. Thus, the extrapolation to infinite He pressure and complete collisional cooling should reveal the percentage, if any, of *trans*-**17** formed directly from *cis*-**16***. Indeed, as Figure 4 shows, the percentage of *trans*-**17** thus formed directly from *cis*-**16*** is 23 $\pm$ 2%. It is also significant that the proportion of *cis*-**17** as a percentage of products is relatively constant across the reaction conditions. This is again consistent with a reaction scheme in which the first reactions of *cis*-**16*** to give products are solely unimolecular and *cis*-**17** is only formed from *cis*-**16***. In summary, the data in Figure 4 show that *cis*-**16*** can undergo collisional cooling back to *cis*-**16** in competition with three unimolecular reactions, forming *trans*-**16**, *cis*-**17** and *trans*-**17**. Extrapolation to 0.0% reaction (full collisional cooling) indicates that the initial unimolecular reactions of *cis*-**16*** give *trans*-**16**, *cis*-**17** and *trans*-**17** in 32 $\pm$ 2%, 45 $\pm$ 1% and 23 $\pm$ 2% yield respectively.

Since *cis*-3-penten-2-ol (**19**) does not undergo elimination under FVP conditions, a six-centered δ-elimination can be ruled out for the direct formation of *trans*-**17** from *cis*-**16***. This leaves the eight-centered δ-elimination as the only mechanistic possibility. This confirms the qualitative prediction that both the six-centered β-elimination and the eight-centered δ-elimination are allowed because they are pseudopericyclic. Indeed, the results in Figure 4 show that these two reactions are competitive, with β-elimination slightly favored over δ-elimination (32 $\pm$ 2% vs 23 $\pm$ 2%).

Computational Results

We had previously reported B3LYP/6−31G(d,p) calculations on model systems, including **3** and **4** (eq 2a and b) that suggested the eight-centered δ-elimination was allowed and might be competitive.[3] These gave us some confidence to pursue the MP-IR experiments described above. We now report a computational study of the potential energy surface for the reactions of *cis*-**16**. Density functional theory (B3LYP/6−31G(d,p) geometry optimization) and *ab initio* calculations (MP4(SDTQ)/cc-pVDZ single point energies) were used to investigate the mechanistic possibilities outlined in Scheme 5 and to explore the pericyclic or pseudopericyclic nature of the reactions.[23,24] The relative energetics are reported in Table 1; in the following discussion, the B3LYP/6−31G(d,p) free energies will be used, unless otherwise indicated. The geometries of the most relevant transition states are presented in Figure 5. The other structures are shown in the Supporting Information.

Table 1. Relative Energies (kcal/mol) and Low or Imaginary Frequencies (cm^{-1}) of Calculated Minima and Transition States in the Reactions of **16** at the B3LYP/6-31G(d,p) Geometry with MP4(SDTQ)/cc-pVDZ Single Point Energies (See Scheme 5)

structure	B3LYP[a] (kcal/mol)	frequency[b] (cm^{-1})	ΔG [c] (kcal/mol)	MP4[d] (kcal/mol)	ΔG MP4[e] (kcal/mol)
cis-**16**	1.2	45.1	1.7	1.0	1.5
trans-**16**	0.0	44.9	0.0	0.0	0.0
***δ*-c-t-TS**	41.2	930.2i	37.5	51.6	47.9
***δ*-c-c-TS**	47.3	1295.8i	44.0	55.9	52.6
***β*-c-c-TS**	43.3	940.7i	38.3	52.3	47.3
***β*-t-t-TS**	41.8	935.5i	36.9	51.3	46.6
3,3-c-t-TS	39.1	414.7i	38.6	43.5	43.0
3,3-c-c-TS	44.9	432.2i	44.5	48.8	48.4
3,3-t-t-TS	36.2	391.5i	35.4	41.5	40.7
HOAc+ *cis*-**17**	15.3		1.4	18.5	4.6
HOAc + *trans*-**17**	13.7		−0.1	17.1	3.3

[a] B3LYP/6−31G(d,p) energy relative to *trans*-**16**. [b] Lowest or imaginary frequency from B3LYP/6−31G(d,p) vibrational calculation. [c] Relative free energy at 298.2 K, based on B3LYP/6−31G(d,p) frequencies. [d] MP4(SDTQ)/cc-pVDZ/B3LYP/6−31G(d,p) relative energies. [e] MP4(SDTQ)/cc-pVDZ/B3LYP/6−31G(d,p) relative energies with B3LYP/6−31G(d,p) free energy corrections.

It is worthwhile to first compare these results with the known experimental and computational results. The racemization of *trans*-**16** is faster than the competitive β-elimination to form *trans*-**17** (eq 5) and rearrangement to *cis*-**16** is even less favored.[16] And indeed, at the B3LYP/6−31G(d,p) level, $\Delta G^{\ddagger}$ (at 298.2 K) is calculated to be 35.4 kcal/mol for the racemization of *trans*-**16** by rearrangement to its enantiomer via **3,3-t-t-TS** (experimental E_a = 38.8 kcal/mol[16]) This compares with 36.9 kcal/mol for the 1,5 elimination via ***β*-t-t-TS** and 38.6 kcal/mol for the rearrangement to *cis*-**16** via **3,3-c-t-TS**. This is reasonable agreement, considering that one reaction involves hydrogen migration from C to O and the other two reactions simply exchange one C−O bond for another. Interestingly, the MP4(SDTQ)/cc-pVDZ calculations (with B3LYP/6−31G(d,p) free energy corrections) give higher barriers for the rearrangements (40.7 and 43.0 kcal/mol) and a much higher barrier for the elimination (46.6 kcal/mol); these calculations are in poorer accord with the experimental results in that the rearrangements and elimination from *trans*-**16** are competitive. The activation energy for elimination of ethyl formate calculated at the B3LYP/6−31G(d,p) level (E_a = 47.4 kcal/mol) is in closer agreement with the experimental barrier (48.3 kcal/mol) than MP2 calculations with various basis sets as reported by Rodríguez-Otero et al.[7e]

Although there are many examples where the B3LYP/6−31G(d,p) level fails to reproduce experimental trends,[25] there are also numerous examples where it gives better agreement with experiment than other levels of theory, particularly for orbital symmetry allowed

(23) Calculations were performed using Gaussian 03.[24] All stationary points were characterized by vibrational frequency analysis and all transition states had a single imaginary frequency. ***β*-SOSP-3** had two imaginary frequencies, as required for a second-order saddle-point. Other constrained geometries were not stationary points. Optimized geometries, absolute energies and further details of the calculations are available in the Supporting Information. Three conformations each of *cis*-**16** and *trans*-**16** were calculated and are reported in the Supporting Information; only the lowest energy ones are discussed in the article.

(24) Frisch, M. J.; et al. *Gaussian 03, Revision C.02*, Gaussian, Inc.: Wallingford CT, 2004. For the full reference, see the Supporting Information.

(25) For a few examples, see: (a) Petersson, G. A.; Malick, D. K.; Wilson, W. G.; Ochterski, J. W.; Montgomery, J. A.; Frisch, M. J. *J. Chem. Phys.* **1998**, *109* (24), 10570–10579. (b) Lynch, B. J.; Truhlar, D. G. *Phys. Chem. A* **2001**, *105*, 2936–2941. (c) Schreiner, P. R.; Fokin, A. A.; Robert, A.; Pascal, J.; Meijere, A. d. *Org. Lett.* **2006**, *8*, 3635–3638. (d) Wodrich, M. D.; Corminboeuf, C.; Schleyer, P. v. R. *Org. Lett.* **2006**, *8*, 3631–3634.

(26) For a few examples, see: (a) Houk, K. N.; Gonzalez, J.; Li, Y. *Acc. Chem. Res.* **1995**, *28*, 81. (b) Wiest, O.; Montiel, D. C.; Houk, K. N. *J. Phys. Chem. A* **1997**, *101*, 8378–8388. (c) Birney, D. M. *J. Am. Chem. Soc.* **2000**, *122*, 10917–10925. (d) Guner, V.; Khuong, K. S.; Leach, A. G.; Lee, P. S.; Bartberger, M. D.; Houk, K. N. *J. Phys. Chem. A* **2003**, *107*, 11445–11459. It is also worth noting that a larger basis set does not necessarily improve the accuracy of B3LYP calculations. (e) Curtiss, L. A.; Raghavachari, K.; Redfern, P. C.; Pople, J. A. *J. Chem. Phys.* **1997**, *106*, 1063–1079.

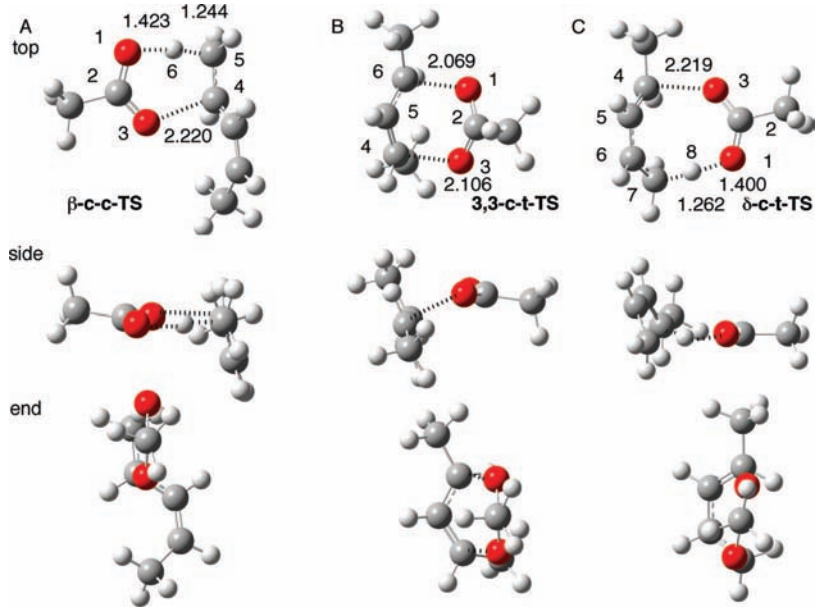

Figure 5. Top, side, and end views of B3LYP/6−31G(d,p) optimized geometries of transition states (A) ***β*-c-c-TS**, (B) **3,3-c-t-TS**, and (C) ***δ*-c-t-TS** for the reactions of *cis*-**16** and *trans*-**16**. Carbons are gray, hydrogens are white and oxygens are red. Distances for breaking and forming bonds are in Ångstroms. The top view is looking above the approximately planar cyclic transition state, the side view is looking at the breaking and forming bonds, and the end view is looking down the acetate CH_3-C bond.

reactions.[26] In this system, the calculated differences between the rearrangements and eliminations at the MP2/6−31G(d,p) level are significant and do not follow the experimental trends; the agreement of the B3LYP/6−31G(d,p) free energies with the experimental trends gives us some degree of confidence in the results.

The B3LYP/6−31G(d,p) free energy calculations also agree with the results of our MP-IR studies on the reaction of *cis*-**16**. Of the five transition states from *cis*-**16** (***δ*-c-t-TS**, ***δ*-c-c-TS**, ***β*-c-c-TS**, **3,3-c-t-TS** and **3,3-c-c-TS**, Scheme 5) the eight-centered elimination via ***δ*-c-t-TS** is calculated to have the lowest activation energy ($\Delta G^{\ddagger}$ = 37.5 kcal/mol). However, the free energy barriers for three reactions that have been shown in these experiments to be competitive (***δ*-c-t-TS**, ***β*-c-c-TS** and **3,3-c-t-TS**) are within about 1 kcal/mol at this level of theory. The other two transition states from *cis*-**16** (***δ*-c-c-TS** and **3,3-c-c-TS**) have higher barriers. The eight-centered elimination to form *cis*-1,3-pentadiene via ***δ*-c-c-TS** is calculated to have a barrier of 44.0 kcal/mol; the degenerate 3,3-rearrangement to form the enantiomer of *cis*-**16** (**3,3-c-c-TS**) has a barrier of 44.5 kcal/mol. These higher calculated barriers justify ignoring these pathways in the discussion of the MP-IR results above.

Experimentally, δ-elimination of acetic acid from *cis*-**16** occurs, as evidenced by our MP-IR studies; B3LYP/6−31G(d,p) calculations suggest this occurs via an eight-centered transition state (***δ*-c-t-TS**). this can be understood as a pseudopericyclic reaction, in which there are one or more orbital disconnections in the cyclic transition state. How well do the calculated transition states agree with this qualitative picture? In the discussion below, we argue that they agree quite well. Moreover, this series of transition states illustrate a more general concept. For reactions where both pseudopericyclic and allowed pericyclic transition state orbital interactions are possible, these can be considered as two electronic states that are of like symmetry. As is the case for other examples of electronic states of like symmetry, they can mix and produce a state of lower energy; the closer in energy the two states are, the more they mix. Thus, if the transition state shows a deviation from the ideal geometry for either a pericyclic or pseudopericyclic reaction, it cannot be purely one or the other, but requires a proportional contribution from each, as we have previously suggested.[1c] There have been significant arguments in the literature[2e−o,p−u] trying to classify reactions as either pericyclic or pseudopericyclic based on transition state aromaticity considerations (NICS[11c,d] or ACID[11e] analysis), although some have also discussed "borderline pseudopericyclic reactions".[2e,j,l] More recently, Chamorro has proposed a scale of pericyclic/pseudopericyclic character for transition states, based on his ELF analysis.[2s] The Atoms in Molecules analysis of Bader[27] has also been explored as a tool for distinguishing the range of these reactions. The ellipticity of the electron density at the bond critical point of the forming bond is more exaggerated in some pericyclic transition states and less so in related pseudopericyclic ones.[21,u] The Laplacian of the electron density (but not the ellipticity) at the bond critical points of the forming bonds has been shown to be different in pericyclic and pseudopericyclic transition states of [4 + 2] cycloadditions.[2v]

To address the pericyclic/pseudopericyclic question for ester eliminations, we first compare the retro-ene reaction of 1-pentene (**5**), a classic six-electron, suprafacial pericyclic reaction[8,11,12] with the β-elimination of formic acid from ethyl formate (**3**)[4] which is allowed either via suprafacial pericyclic (as described in the literature[5−7]) or planar pseudopericyclic transition states.[1−3] The transition state geometries of these (***β*-TS-5** and ***β*-TS-3**) are significantly different, as shown in Table 2 and Figure 6.

The transition state (***β*-TS-5**) for the retro-ene reaction of **5** has been calculated at a number of theoretical levels[8] including B3LYP/6−31G(d)[8b] and CASPT2.[8c] The geometries are similar at all levels. The B3LYP/6−31G(d)[8b] transition state is reproduced in Figure 6E; the barrier for the retro-ene is 58.1 kcal/mol at this level.[8b] Selected occupied molecular orbitals (MOs) and natural bond orbitals[28] (NBOs) are shown in Figure S3 (Supporting Information) and clearly reflect the qualitative orbital picture in Figure 1A. The breaking σ-bonds are nearly coplanar, as required for the formation of the new C4−C5 π-bond; the C3−C4−C5−H6 dihedral angle is 11.7°. As also required for suprafacial orbital overlap in the allyl π-system, the allyl fragment is tipped far out of the plane of the breaking σ-bonds; the dihedral angles C1−C2−C3−C4 and

(27) Bader, R. F. *Atoms in Molecules - A Quantum Theory; number 22 in The International Series of Monographs on Chemistry*; Oxford University Press: Oxford, 1990.
(28) (a) Weinhold, F.; Carpenter, J. E. *The Structure of Small Molecules and Ions*; Plenum: New York, 1988. (b) Reed, A. E.; Curtiss, L. A.; Weinhold, F. *Chem. Rev.* **1988**, *88*, 899–926.

Table 2. Selected Dihedral Angles of Transition States Calculated at the B3LYP/6-31G(d,p) Level, unless Otherwise Indicated[a]

	dihedral						
Structure	1234	2347	3478			8123	
δ-c-t-TS	7.9	−13.8	10.9			4.1	
δ-c-c-TS	−2.8	4.8	−1.6			−4.4	
	1234	2345	3456	4561	5612	6123	3461
β-c-c-TS	−5.5	−3.1	−6.3	[g]	[g]	7.1	
β-t-t-TS	−6.3	−3.1	6.7	[g]	[g]	8.1	
3,3-c-t-TS	37.3	9.4	−64.7	66.4	−14.0	−34.8	1.7
3,3-c-c-TS	43.6	−0.6	−59.2	66.4	−16.4	−35.1	6.6
3,3-t-t-TS	33.3	13.9	−65.9	65.9	−13.9	−33.3	0.0
β-TS-5[b]	−63.5	37.6	11.7	[g]	[g]	57.3	
β-TS-3[c] B3LYP	0.0	0.0	0.0	[g]	[g]	0.0	
β-TS-3[d] MP2	−32.7	8.1	8.9	[g]	[g]	30.2	
β-SOSP-3[e] MP2	0.0	0.0	0.0	[g]	[g]	0.0	
β-ene-3[f] MP2	−63.5	27.3	1.0	[g]	[g]	57.3	

[a] Atom numbering is as in Figures 5 and 6. [b] B3LYP/6−31G(d) optimization, from ref 8b. [c] B3LYP/6−31G(d,p) tight optimization. [d] MP2/6−31G(d,p) geometry from ref 7d. [e] This planar structure is a second-order saddle point at the MP2/6−31G(d,p) level. [f] MP2/6−31G(d,p) optimized with the 1234 and 6123 dihedral angles constrained to −63.5° and 57.3° respectively (from ***β*-TS-5**). [g] Because the partial bonds to H6 are nearly linear, the 4561 and 5612 dihedral angles are not particularly meaningful.

C3−C2−C1−H6, are −63.5 and 57.3°, respectively. These are similar to the corresponding dihedral angles in other typical hydrocarbon transition states. For example, in the Cope reaction of 1,5-hexadiene this angle is 65.1° at the B3LYP/6−31G(d) level[29] and in the transition state for Diels−Alder reaction between 1,3-cyclohexadiene and quinone, this dihedral angle is 64.6° at the B3LYP/6−31G(d,p) level.[30]

The transition state for β-elimination of ethyl formate at the B3LYP/6−31G(d,p) level has been variously reported to have a planar[7b] or a slightly nonplanar geometry.[7e] We started from a nonplanar geometry and performed an optimization at the B3LYP/6−31G(d,p) level with tight optimization cutoffs; this reproduces the planar structure[7b] (***β*-TS-3**, O1−C2−O3−C4 and H6−O1−C2−O3 dihedrals of 0.0°) shown in Figure 6A. The HOMO and HOMO-1 are shown in Figure 1C,D; other selected occupied MOs and NBOs[28] are shown in the Supporting Information and clearly reflect the qualitative orbital picture in Figure 1B. The calculated barrier is 50.4 kcal/mol; this is lower than that calculated for **5**, as expected when comparing pseudopericyclic and pericyclic reactions. The MP2 method with a variety of basis sets predicts slightly nonplanar transition states[3,7e,31] that are close in energy to the planar second-order saddle point (***β*-SOSP-3**), only 0.2 kcal/mol more stable at the MP2/6−31G* and G2(MP2) levels.[3] Figure 6 shows the MP2/6−31G(d,p) nonplanar structure[7e] (***β*-TS-3**, Figure 6C) and the planar structure (***β*-SOSP-3**, Figure 6B); the latter is still only 0.2 kcal/mol higher in energy.

We also performed a constrained transition state optimization (***β*-ene-3**, Figure 6D) at the MP2/6−31G(d,p) level that is analogous to the retro-ene reaction of 1-pentene, fixing the O1−C2−O3-C4 and H6−O1−C2-O3 dihedral angles to −63.5° and 57.3°, which are those calculated for ***β*-TS-5** at the B3LYP/6−31G(d,p) level. This nonstationary point (***β*-ene-3**) is calculated to be 4.2 kcal/mol higher in energy (without free energy corrections) than ***β*-TS-3**. Distorting toward the nonplanar Woodward−Hoffmann suprafacial orbital topology in ***β*-ene-3** requires substantially more energy than does the distortion to the planar, pseudopericyclic orbital topology in ***β*-SOSP-3**. This suggests that the MP2/6−31G(d,p) transition state ***β*-TS-3** is primarily stabilized by the pseudopericyclic interactions, even though the pericyclic interactions are slightly manifest in the transition state geometry.

Returning to the transition states for the eight-centered δ-eliminations of acetic acid from *cis*-**16** (***δ*-c-t-TS**, Figure 5C and ***δ*-c-c-TS**, Supporting Information), these would be forbidden if they had the same orbital topology as the retro-ene of 1-pentene (***β*-TS-5**). They would be allowed if they were pericyclic and antarafacial on one component or alternatively if they were pseudopericyclic. The acetate fragment is nearly coplanar with the breaking C−O bond and the forming O−H bond; the O1−C2−O3−C4 dihedrals are 7.9 and −2.8° and the H8−O1−C2−O3 dihedrals are 4.1 and −4.4° respectively. Interestingly, the acetate fragments are very slightly twisted toward the geometry that would be required for antarafacial overlap[12] (Mobiüs aromaticity)[11] of the acetate fragment with the breaking and forming bonds, as seen in the end view of ***δ*-c-t-TS** in Figure 5C. Constraining these dihedral angles to 0.0° in ***δ*-c-t-TS** raises the energy by an inconsequential amount, 0.1 kcal/mol (Table S4, Supporting Information); the calculated free energy of ***δ*-c-t-TS** is lower by 0.1 kcal/mol at this nonstationary point. Based on these energetics, this is essentially a purely pseudopericyclic reaction. The near planarity of the transition states is consistent with the qualitative geometry expected for a pseudopericyclic transition state in which the breaking and forming bonds are in the plane of the acetate fragment. The molecular orbitals are likewise consistent with a pseudopericyclic transition state, showing a clear separation between the acetate π- and σ-systems (Figure S4, Supporting Information). The breaking C−O and C−H σ-bonds are close to coplanar; the O3−C4−C7−H8 dihedral angles are 10.9 and −1.6° respectively, as expected for the formation of the new diene π-bond system.

The geometries of the transition states for the β-eliminations (***β*-c-c-TS** and ***β*-t-t-TS**) are not quite as planar as the pseudopericyclic δ-eliminations (***δ*-c-c-TS**, and ***δ*-c-t-TS**). The O1−C2−O3−C4 dihedrals are −5.5 and −6.3° and the H6−O1−C2−O3 dihedrals are 7.1 and 8.1° in ***β*-c-c-TS** and ***β*-t-t-TS** respectively, indicating a distortion toward suprafacial orbital overlap on the acetate fragment. This can be seen in the end view of ***β*-c-c-TS** in Figure 5A; note that both of the breaking and forming bonds are to the same side of the acetate fragment. This must mean that the transition states are not purely pseudopericyclic. However, these geometries are far from being as significantly out-of-plane as the retro-ene reaction transition state (***β*-TS-5**), as discussed above, and so ***β*-c-c-TS** and ***β*-t-t-TS** are not purely pericyclic either.

The geometries of the [3,3]-sigmatropic rearrangements are more distorted toward a pericyclic transition state than are the β- or δ-eliminations. For **3,3-c-t-TS**, **3,3-c-c-TS**, and **3,3-t-t-TS**, the O1−C2−O3−C4 dihedrals are 37.3, 43.6, and 33.3° and the C6−O1−C2−O3 dihedrals are −34.8, −35.1, and −33.3°, respectively. These compare well with the angles calculated at the MP2/6−31G(d) level for allyl formate [3,3]-rearrangement boat transition state.[32] However, these angles are still far from those in a hydrocarbon Cope reaction (65.1° at the B3LYP/6−31G(d) level).[29] As might be expected, constraining **3,3-c-t-TS** to a planar geometry raises the energy a bit more, this nonstationary point is 1.6 kcal/mol higher in energy (Table S4, Supporting Information).

In the discussion above, geometry and energy have been used to compare pericyclic and pseudopericyclic contributions to the transition states. Are the calculated transition state aromaticities consistent as well? The nucleus independent chemical shift (NICS) has been used to provide a quantitative measure of aromaticity in both ground and transition states.[11c,d] In the simplest systems, the

(29) Wiest, O.; Black, K. A.; Houk, K. N. *J. Am. Chem. Soc.* **1994**, *116*, 10336–10337.
(30) Birney, D.; Lim, T. K.; Koh, J. H. P.; Pool, B. R.; White, J. M. *J. Am. Chem. Soc.* **2002**, *124*, 5091–5099.
(31) MP2 calculations on pericyclic reactions often give activation energies that are lower than experiment.[26]
(32) Pascal, Y. L.; Levisalles, J.; Normant, J.-M. *Tetrahedron* **1993**, *49*, 7679–7690. A chair transition state is also found for the rearrangement of allyl formate; this is 1.9 kcal/mol higher in energy than the boat transition state at the MP2/6−31G* + ZPE level. Attempts to locate a chair transition state corresponding to **3,3-c-t-TS** were unsuccessful at the B3LYP/6−31G(d,p) level; the optimizations proceeded smoothly to give **3,3-c-t-TS**.

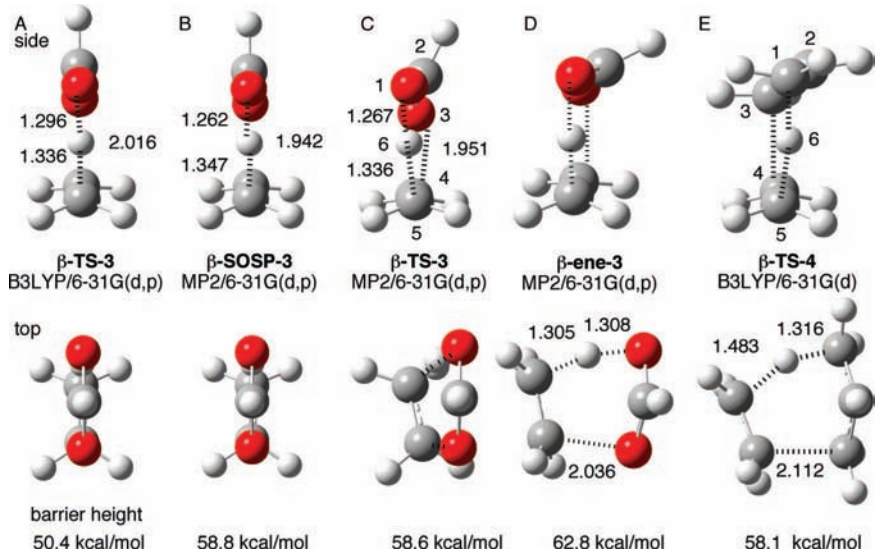

Figure 6. Side and top views of calculated transition states. (A) ***β*-TS-3** (B3LYP/6−31G(d,p), tight optimization, compare with refs 7b [planar] and 7e [nonplanar]), (B) MP2/6−31G(d,p) second order saddle point (***β*-SOSP-3**, this work), (C) MP2/6−31G(d,p) transition state (***β*-TS-3**, reproduced from ref 7e), (D) MP2/6−31G(d,p) constrained to the 1234 and 3216 dihedral angles of −63.5° and 57.3° respectively, corresponding to those of ***β*-TS-5**. This is a transition state within the constraints, but is not a stationary point. (E) ***β*-TS-5** (B3LYP/6−31G(d), reproduced from ref 8b). See Figure 5 for key. Barrier heights are at the corresponding level of theory without any vibrational corrections.

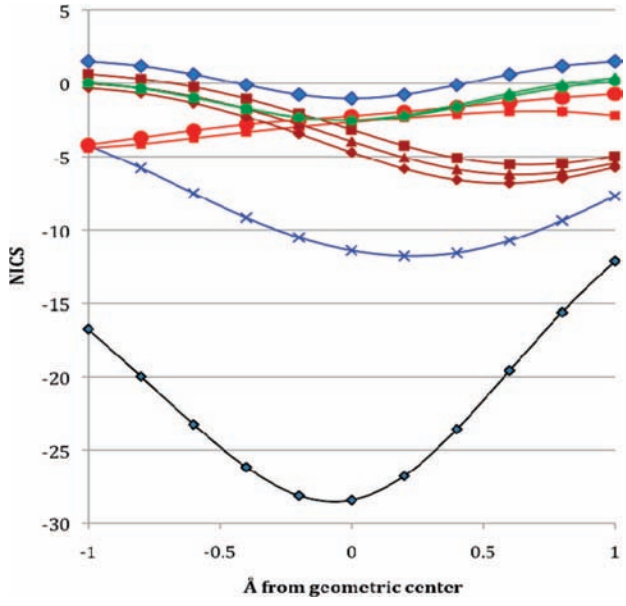

Figure 7. NICS values calculated for the indicated transition states. See text for a description of the calculations. Key ***β*-TS-5** black ♦, ***β*-TS-3** blue ♦, ***β*-ene-3** blue ×, ***δ*-c-t-TS** red ●, ***δ*-c-c-TS** red ■, **3,3-c-t-TS** burgandy ▲, **3,3-c-c-TS** burgandy ♦, **3,3-t-t-TS** burgundy ■, ***β*-c-c-TS** green ▲, ***β*-t-t-TS** green ●.

chemical shift is evaluated at the center of the aromatic ring and at points above and below the plane of that ring. This is complicated by the lack of symmetry and nonplanar geometry of many transition states. In this work, the center was taken as the geometric center of the four heavy atoms (C, O) with partial ***σ***-bonds. The chemical shift was then evaluated at five points 0.2 Å apart above and below the approximate plane defined by these four atoms. The results (RHF/6−31+G(d) GIAO) are summarized in Figure 7. The retro-ene reaction of 1-pentene (***β*-TS-5**) shows a typical pattern for a pericyclic transition state,[11c,d] with significant aromaticity (a minimum NICS value of −28). Constraining the ethyl formate elimination to a similar geometry (***β*-ene-3**) shows less, but still significant transition state aromaticity (a minimum NICS value of −12); this is consistent with some pseudopericyclic orbital overlap at this geometry as well. The β-and δ-eliminations of the esters have low transition state aromaticitity (minimum NICS value ≤ -3 and ≤ -5, respectively). The δ-eliminations have more negative NICS values on the side near the alkene carbons (C6 and C6); the NICS value at the center of the ring is ≤ -3), comparable to the β-eliminations. The 3,3-rearrangements (**3,3-c-c-TS**, **3,3-c-t-TS**, and **3,3-t-t-TS**) show slightly more transition state aromaticity and are more distorted out of plane than the eliminations. Even here, the most negative points are near the central allyl carbon (C5, Figure 5); the NICS values at the center of the ring are smaller, while constraining the reaction to be planar on the acetate (**3,3-c-t-TS-planar**) makes the reaction substantially less aromatic (minimum NICS value −1, Figure S7, Supporting Information). When the slightly nonplanar elimination transition states (***β*-SOSP-3** and ***δ*-c,t-TS-planar**) are constrained to be planar on the acetate, the NICS curves are quite close (Figure S7, Supporting Information). These NICS results are consistent with the argument that the pseudopericyclic reactions lack the transition state aromaticity of pericyclic reactions. They also tend to support the suggestion that pericyclic and pseudopericyclic orbital topologies can mix, giving rise to transition states that are likewise mixed.

Conclusions

(1) MP-IR of *trans*-**16** at 1057.3 cm^{-1} gives rearrangement to *cis*-**16** and elimination to a mixture *cis*- and *trans*-**17**. However, adding He buffer gas increases the yield of *cis*-**16**, and concomitantly reduces the formation of *cis*-**17**. Extrapolation to complete cooling indicates that essentially all of the formation of *cis*-**17** is stepwise, by rearrangement from *trans*-**16*** to *cis*-**16*** and then elimination to *cis*-**17**, while all of the *trans*-**17** is formed directly from *trans*-**17***.

(2) Similarly, MP-IR of *cis*-**16** at 1057.3 cm^{-1} gives rearrangement to *trans*-**16** and elimination to a mixture *cis*- and *trans*-**17**. Adding He buffer gas increases the yield of *trans*-**16**, and concomitantly reduces the formation of *trans*-**17**. However, extrapolation to complete cooling indicates that approximately 23% of the observed *trans*-**17** is formed directly from *cis*-**16**, while 45% of the reaction directly forms *cis*-**17** and 32% forms *trans*-**16**. The remainder of the observed *trans*-**17** is formed by the stepwise process, rearrangement from *cis*-**16*** to *trans*-**16***,

followed by elimination to *trans*-**17**. Significantly, this work demonstrates that *cis*-**16*** undergoes rearrangement in competition with both β- and δ-eliminations. Because alcohol **19** does not eliminate under the flash vacuum conditions that decompose *cis*-**16**, the δ-eliminations arguably occurs via an eight-centered transition state. Qualitative considerations suggest that both the β- and δ-eliminations are pseudopericyclic.

(3) The general trends in the barrier heights for the competing reactions of *cis*-**16** and *trans*-**16** are better reproduced by transition state calculations at the B3LYP/6−31G(d,p) level than at the MP4(SDTQ)/cc-pVDZ//MP2/6−31G(d,p) level. The transition state geometries for the δ-eliminations, ***δ*-c-c-TS**, and ***δ*-c-t-TS**, are essentially planar on the acetate fragment. The molecular orbitals and the Natural Bond Orbitals show a clear σ, π-separation. Constraining ***δ*-c-t-TS** to a planar geometry raises the energy by an inconsequential 0.1 kcal/mol. The NICS values are small, as compared to more pericyclic β-eliminations (***β*-TS-5** and ***β*-ene-3**). These are all consistent with δ-eliminations being primarily pseudopericyclic.

(4) The calculated transition state geometries for β-eliminations of esters are either planar, as for ethyl formate (***β*-TS-3**) at the B3LYP/6−31G(d,p) level, or slightly nonplanar, as for ***β*-TS-3** at the MP2/6−31G(d,p) level and ***β*-c-c-TS**, and ***β*-t-t-TS** at the B3LYP/6−31G(d,p) level. The NICS values are very small. The planar ethyl formate second order saddle point (***β*-SOP-3**) is only slightly higher in energy (0.2 kcal/mol) than the nonplanar transition state, but constraining the dihedral angles to those of the hydrocarbon ene reaction raises the energy by 4.0 kcal/mol. The geometric, energetic and aromaticity criteria are consistent with these as pseudopericyclic reactions.

(5) The calculated boat transition state geometries for the [3,3]-rearrangements (**3,3-c-c-TS**, **3,3-c-t-TS** and **3,3-t-t-TS**) are the furthest from a planar, pseudopericyclic geometry. However, these are far from the nonplanar transition state geometries calculated for the hydrocarbon Cope rearrangement. Constraining **3,3-c-t-TS** to planarity raises the energy by a modest 1.6 kcal/mol. The NICS values are still relatively small. These calculations are also consistent with primarily pseudopericyclic transition states.

(6) We suggest that in general, when both a pseudopericyclic and a pericyclic orbital topology are possible for a reaction, the transition state can involve mixing of these two electronic states. The degree of mixing can be manifest in the energy of the transition state, as compared to that of either of the ideal transition states. The geometry can likewise provide an indication of the degree of mixing of prototypical pseudopericyclic (planar) and pericyclic (nonplanar) allowed transition states. Indeed, we suggest that any transition state property should reflect this mixing.

Acknowledgment. This work was supported by grants from the Robert A. Welch Foundation and the National Science Foundation (0415622). We thank Ms. Emily Jenkins for assistance with preliminary calculations. D.M.B. thanks Professor Peter Chen and his group members for hospitality during a development leave and Dr. Erik Pieter Adriaan Couzijn for helpful discussions.

Supporting Information Available: Experimental details for synthesis and MP-IR of *cis*-**16** and *trans*-**16**. Computational details including absolute energies and Cartesian coordinates of all optimized structures. Complete ref 24. This material is available free of charge via the Internet at http://pubs.acs.org.

JA804812C